

Large potential steps at weakly interacting metal-insulator interfaces

Menno Bokdam,^{*} Geert Brocks, and Paul J. Kelly

Faculty of Science and Technology and MESA⁺ Institute for Nanotechnology,
University of Twente, P.O. Box 217, 7500 AE Enschede, The Netherlands

(Dated: September 13, 2021)

Potential steps exceeding 1 eV are regularly formed at metal|insulator interfaces, even when the interaction between the materials at the interface is weak physisorption. From first-principles calculations on metal|*h*-BN interfaces we show that these potential steps are only indirectly sensitive to the interface bonding through the dependence of the binding energy curves on the van der Waals interaction. Exchange repulsion forms the main contribution to the interface potential step in the weakly interacting regime, which we show with a simple model based upon a symmetrized product of metal and *h*-BN wave functions. In the strongly interacting regime, the interface potential step is reduced by chemical bonding.

PACS numbers: 73.30.+y, 73.40.Ns

Introduction.—The potential step that is formed at the interface between a metal and a semiconductor or insulator is an essential physical parameter determining device performance [1]. A satisfactory understanding of the factors influencing the step is complicated by its extreme sensitivity to interface structure and disorder [1]. Metal contacts with the layered van der Waals (vdW) structures that are the subject of much current study [2], in particular hexagonal boron nitride (*h*-BN) [3], form an ideal model system to study such metal contacts. Because *h*-BN is chemically unreactive, it can form essentially defect-free interfaces with metals making possible a particularly clean confrontation of theory with experiment. Potential steps involving *h*-BN are already very interesting in their own right [2, 3].

The formation of an interface between metals and 2D materials such as graphene or *h*-BN leads to a dipole layer and a potential step at the interface [4–7]. Naively, one might expect the interface dipole and potential step to be small if the interaction between the two materials is weak. It is then puzzling to find that physisorption of graphene or *h*-BN on metal substrates, with adsorption energies as small as ~ 0.05 eV/atom [8, 9], leads to substantial potential steps ΔV of ~ 1 eV [10, 11], see Figure 1. A possible explanation for a large potential step is direct transfer of electrons across the interface, which occurs on equilibrating the chemical potential between two conductors. This happens at metal|graphene interfaces, for instance, and results in doping of graphene; the corresponding contribution to the potential step is Δ_{tr} [10]. For graphene there is an additional, large contribution to the total potential step arising from the direct (physisorption) interaction at the interface. That contribution, called Δ_c in Ref. 10, was found to depend roughly exponentially on the graphene-metal distance, underlining its local, interface character. Thus, for graphene,

$\Delta V = \Delta_{\text{tr}} + \Delta_c$. Similar terms were identified in Ref. 12. Direct charge transfer cannot occur across a metal|*h*-BN interface because *h*-BN is a wide band gap insulator. Yet even here large potential steps are found [7, 11, 13, 14]. The absence of direct charge transfer makes it possible to study the potential step arising from just the interface interaction.

In this paper, we use first-principles calculations to explore the origin of the interface dipole and potential step at metal|insulator interfaces. We focus on metal|*h*-BN as an archetypal interface, selecting in particular those cases where the bonding interaction at the interface is weak. Surprisingly, the interface potential step does not depend on the exchange-correlation functional used to calculate it, even though the binding energy curve is quite sensitive to that functional as shown by Fig. 1. This points

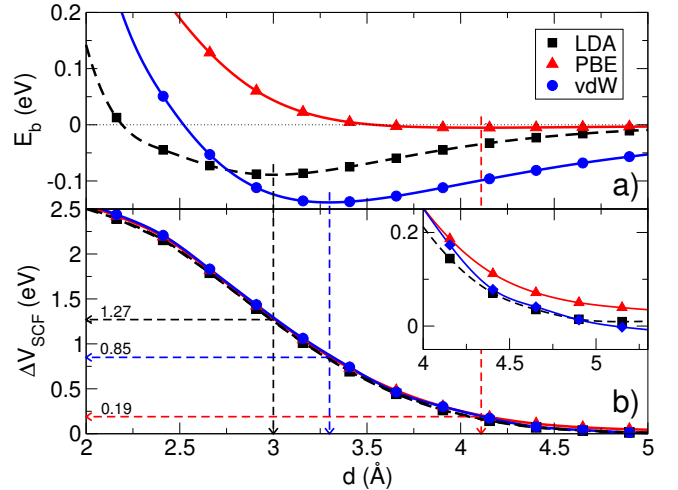


FIG. 1. (color online) (a) Binding energy curves $E_b(d)$ in eV/BN for a monolayer of *h*-BN on Cu(111) calculated with LDA (black squares), GGA-PBE (red triangles), and optB88-vdW-DF (blue circles) functionals. The vertical dashed lines indicate the minima. (b) The corresponding interface potential steps $\Delta V_{\text{SCF}}(d)$ calculated with the three functionals.

^{*} Current address: Faculty of Physics, University of Vienna, Computational Materials Physics, Sensengasse 8/12, 1090 Vienna, Austria.

to a more general origin of the potential step. From a transparent model based upon a symmetrized product of fragment states, we show that exchange repulsion at the interface between the metal and the insulator is the main source of the potential step. The van der Waals bonding between the two materials gives a much smaller contribution.

Interactions between closed-shell molecules or ions give rise to dipoles with an exponential separation dependence [15]. This behavior is ascribed to Pauli repulsion which pushes electrons out of the overlap region between molecules and results in a distortion of the electron distribution. The dipoles that are formed when inert atoms or molecules adsorb on metal surfaces are also attributed to Pauli repulsion. In this context, the occurrence of such dipoles is called the push-back or pillow effect [12, 16]. In the following, we demonstrate the effect of the Pauli repulsion explicitly by calculating its contribution to the potential steps at weakly interacting metal|*h*-BN interfaces.

DFT calculations.—The potential step at an A|B metal|insulator interface is obtained from self-consistent calculations as the difference between the work functions W of the clean metal surface, W_A , and of the combined system; $\Delta V_{\text{SCF}} = W_A - W_{\text{A|B}}$ [17]. Here we adsorb a *h*-BN monolayer on close-packed (111) metal surfaces. We consider commensurate interfaces, accommodating lattice mismatch by adapting the in-plane lattice constant of the metals to that of *h*-BN so that the strain remains < 5%, as in Refs. 10 and 11. Changing the lattice constant of a metal by a few percent changes its electronic properties only mildly, whereas adapting the lattice constant of *h*-BN is a much larger perturbation. Weakly interacting metal|*h*-BN interfaces are found to exhibit in-plane moiré patterns with large periods. Calculations for such in-plane superstructures are computationally very demanding and are not crucial for the present study. A more detailed discussion of the effects of incommensurability can be found in Refs. 18 and 19.

For the DFT calculations we use the Vienna Ab-initio Simulation Package (VASP) [20], and follow Ref. 11 concerning interface structures and choice of computational parameters. We consider three different functionals: the local density approximation (LDA) [21], the PBE generalized gradient approximation (GGA) [22], and a van der Waals density functional [23–25]. Though it generally overestimates chemical interactions, the LDA gives a reasonable description of the binding energy and equilibrium separation of metal|*h*-BN interfaces [19]. GGA often gives a good description of chemisorption but fails to capture physisorption. Local or semi-local functionals lack vdW interactions which play an important role in physisorption [26] and in the bonding of layered materials [27]. These interactions are modeled in non-local vdW functionals. Here we use the optB88-vdW-DF functional [25], which has been shown to give a good description of graphene on Ni [28].

Figure 1(a) shows the binding energy curves of *h*-BN

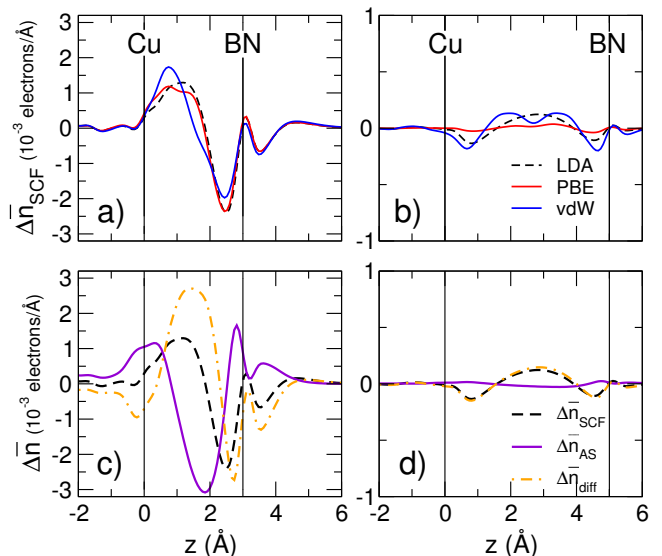


FIG. 2. (color online) The plane-averaged electron displacements from self-consistent calculations $\Delta\bar{n}_{\text{SCF}}(z)$ at (a) $d = 3$ Å and (b) $d = 5$ Å. (c) Comparison of $\Delta\bar{n}_{\text{SCF}}$ (LDA: black dashed) with $\Delta\bar{n}_{\text{AS}}$ of the corresponding AS state calculated using Eq. (4) (violet); and their difference $\Delta\bar{n}_{\text{diff}}$ (orange dash-dotted) referred to as the bonding contribution, for a Cu(111)-*h*-BN separation of 3 Å and (d) 5 Å.

on Cu(111) for the three functionals. GGA gives essentially no bonding, with an adsorption energy $E_b = -1$ meV/BN at an equilibrium separation $d_{\text{eq}} = 4.1$ Å; LDA gives a reasonable bonding with $E_b = -87$ meV/BN at $d_{\text{eq}} = 3.0$ Å; optB88-vdW-DF gives $E_b = -140$ meV/BN at $d_{\text{eq}} = 3.3$ Å, underlining the importance of vdW interactions [29, 30]. Whereas the binding energy curves evidently depend sensitively on the (type of) functional used [31], the interface potential step is remarkably insensitive. This is clearly demonstrated in Fig. 1(b) where the potential step at the Cu(111)|*h*-BN interface, ΔV_{SCF} , is shown as a function of the separation d between the Cu(111) surface and the *h*-BN plane. The curves for the three functionals are within 0.05 eV of one another.

The potential step is proportional to the interface dipole which can be derived from the electron displacement $\Delta n_{\text{SCF}} = n_{\text{A|B}} - n_A - n_B$, where $n_{\text{A|B}}$, n_A , and n_B are, respectively, the electron densities of the metal|*h*-BN system, the isolated metal, and the *h*-BN monolayer. The insensitivity of the potential step to the functional suggests a similar insensitivity of Δn_{SCF} , which is confirmed by Figs. 2(a) and (b). At $d = 3$ Å, i.e., close to the (experimental) equilibrium separation proposed in Ref. 7, $\Delta V_{\text{SCF}} \approx 1$ eV, and the plane-averaged electron displacement, $\Delta\bar{n}_{\text{SCF}}(z)$, is very similar for all three functionals. At a larger separation, $d = 5$ Å, $\Delta\bar{n}_{\text{SCF}}$ for the vdW-DF functional shows an accumulation of electrons between the top metal plane and the *h*-BN sheet, and a depletion closer to these.

Such a pattern is also observed in an (Ar)₂ vdW com-

plex, suggesting that this is typical for vdW interactions [24]. Indeed this pattern is absent from the PBE $\Delta\bar{n}_{\text{SCF}}$ at $d = 5 \text{ \AA}$. Interestingly, $\Delta\bar{n}_{\text{SCF}}$ calculated with the LDA is quite similar to that found for the vdW-DF. A local functional cannot represent vdW interactions properly, hence the substantial differences between the LDA and the vdW-DF binding energy curves. Nevertheless, it is remarkable that both the LDA and vdW-DF give very similar electron distributions. At $d = 5 \text{ \AA}$, $\Delta V_{\text{SCF}} < 0.05 \text{ eV}$, demonstrating that vdW interactions as such do not give rise to large interface dipoles.

Model.—The insensitivity of the dipole to the functional used suggests a model that does not rely heavily upon the specific functional. An approximation to the ground state of an A|B interface should be a fermion state. Starting from two well-separated systems A and B, a simple fermion state is the antisymmetrized product

$$|\Psi\rangle = \hat{A}\hat{B}|0\rangle, \quad (1)$$

where

$$\hat{X} = \prod_{\mathbf{kn} \in \text{occ}} \hat{c}_{X,\mathbf{kn}}^\dagger; \quad X = A, B, \quad (2)$$

with $|0\rangle$ the vacuum, \mathbf{kn} the Bloch vector and band index. The fermion operator $\hat{c}_{X,\mathbf{kn}}^\dagger$ creates an electron in the orbital $|\phi_{\mathbf{kn}}^X\rangle$, and the product is over all occupied states. The state $|\Psi\rangle$ incorporates the exchange of electrons among any of the occupied orbitals of A and B. We take it to define the Pauli exchange interaction between systems A and B, and refer to this state as the anti-symmetrized (AS) product state.

If the orbitals on A and B overlap at the interface between the two systems, they are in general not orthogonal. The technical difficulties of calculating expectation values with non-orthogonal orbitals can be circumvented. Define a linear transformation, $\hat{c}_\beta^\dagger = \sum_\alpha \hat{c}_\alpha^\dagger T_{\alpha\beta}$, where α or β is a short-hand notation for the combined index (X, \mathbf{kn}) that runs over all occupied states of both systems A and B. The same transformation defines new orbitals, $|\phi'_\beta\rangle = \sum_\alpha |\phi_\alpha\rangle T_{\alpha\beta}$. The state $|\Psi\rangle$ is invariant under such a transformation, apart from a multiplicative factor, $|\Psi'\rangle = \det(T)|\Psi\rangle$, which follows directly from its definition, Eqs. (1) and (2). Orthogonalizing the orbitals $\langle\phi'_\alpha|\phi'_\beta\rangle = \delta_{\alpha\beta} = \sum_{\gamma,\zeta} T_{\gamma\alpha}^* S_{\gamma\zeta} T_{\zeta\beta}$, where $S_{\gamma\zeta} = \langle\phi_\gamma|\phi_\zeta\rangle$ is the overlap matrix of the original orbitals, defines a transformation that reads in matrix form $\mathbf{I} = \mathbf{T}^\dagger \mathbf{S} \mathbf{T}$, or $\mathbf{T} \mathbf{T}^\dagger = \mathbf{S}^{-1}$. The expectation value with respect to $|\Psi\rangle$ of any operator can then be calculated using the standard expressions for orthogonal orbitals. For instance, for any single-particle operator one obtains $\sum_\alpha \langle\phi'_\alpha|\hat{o}|\phi'_\alpha\rangle = \sum_{\alpha,\beta} \langle\phi_\alpha|\hat{o}|\phi_\beta\rangle S_{\beta\alpha}^{-1}$.

The density operator $\hat{n}(\mathbf{r}) = |\mathbf{r}\rangle\langle\mathbf{r}|$ is an example of a single-particle operator, whose expectation value is the electron density

$$n_{\text{AS}}(\mathbf{r}) = \sum_{\alpha,\beta} \phi_\alpha^*(\mathbf{r})\phi_\beta(\mathbf{r})S_{\beta\alpha}^{-1}, \quad (3)$$

with $\phi_\alpha(\mathbf{r}) \equiv \langle\mathbf{r}|\phi_\alpha\rangle$. We define the electron displacement $\Delta n_{\text{AS}}(\mathbf{r})$ as the change in the electron density of the combined AB system with respect to the sum of the electron densities of the two separate systems, A and B,

$$\Delta n_{\text{AS}}(\mathbf{r}) = \sum_{\alpha,\beta} \phi_\alpha^*(\mathbf{r})\phi_\beta(\mathbf{r}) \left(S_{\beta\alpha}^{-1} - \delta_{\beta\alpha} \right). \quad (4)$$

The double sum is over all occupied orbitals (X, \mathbf{kn}) . The overlap matrix and its inverse are block-diagonal in \mathbf{k} , but not in the system and band indices X, n .

By construction, $\int \Delta n_{\text{AS}}(\mathbf{r})d^3r = 0$ (integrated over all space). If the overlap between the A and B subsystems is confined to an interface, then $\Delta n_{\text{AS}}(\mathbf{r}) \rightarrow 0$ away from the interface. Solving the Poisson equation with $\Delta n_{\text{AS}}(\mathbf{r})$ as source then yields a step in the potential (energy) across the interface. Averaging $\Delta n_{\text{AS}}(\mathbf{r})$ over planes yields $\Delta\bar{n}_{\text{AS}}(z)$ in terms of which the step $\Delta V_{\text{AS}} = \frac{e^2}{\epsilon_0} \int_{-\infty}^{\infty} z \Delta\bar{n}_{\text{AS}}(z) dz$ can be defined, with z the direction normal to the interface.

Cu(111)|h-BN interface.—Figure 3 shows ΔV_{AS} calculated for the Cu(111)|h-BN interface with the AS state constructed as discussed above as a function of d , the separation between the Cu(111) surface and the h-BN plane. ΔV_{AS} is an exponential function of d , consistent with the fact that it depends on the overlap between the Cu and the h-BN wave functions at the interface. The behavior of the potential step obtained from fully self-consistent calculations, ΔV_{SCF} , is slightly more complicated. For separations $d \geq 3.4 \text{ \AA}$, ΔV_{SCF} coincides with ΔV_{AS} . In this regime exchange repulsion between Cu(111) and h-BN provides a good description of the interface potential step.

For separations $d \lesssim 3.4 \text{ \AA}$, ΔV_{SCF} deviates from ΔV_{AS} . At these shorter distances, stronger (chemical) interactions between the two systems become dominant, resulting in a more drastic change of the electronic states and in departure from simple exponential behavior. At the

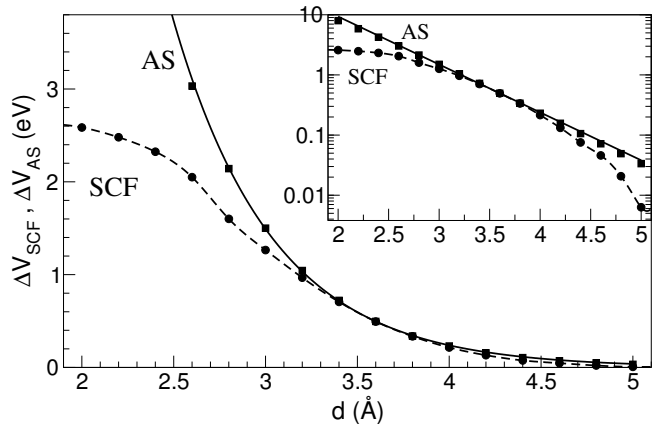


FIG. 3. Potential steps ΔV_{SCF} , ΔV_{AS} at the Cu(111)|h-BN interface from self-consistent LDA calculations and from the AS state, Eq. (1), respectively. Inset: potential steps on a logarithmic scale.

vdW-DF equilibrium separation, $d_{eq} = 3.3\text{\AA}$, the potential step calculated from exchange repulsion is only $\sim 5\%$ higher than the SCF value. At the LDA equilibrium separation, $d_{eq} = 3.0\text{\AA}$, exchange repulsion overestimates the SCF value by $\sim 25\%$. For distances $d \gtrsim 4.0\text{\AA}$ ΔV_{SCF} also starts to deviate from ΔV_{AS} . This is caused by the long range vdW interaction between Cu(111) and *h*-BN. Note however that at these distances $\Delta V_{SCF} < 0.1\text{ eV}$, so the impact of the long range interactions is in absolute terms small.

The plane-averaged electron displacement calculated with the AS state, $\Delta\bar{n}_{AS}(z)$, is plotted in Fig. 2 (c)-(d). Exchange repulsion pushes electrons out of the overlap region between the Cu(111) surface and the *h*-BN plane. The system as a whole stays neutral, and the depleted electrons are accumulated close to the Cu(111) surface and the *h*-BN plane. The depletion/accumulation pattern is asymmetric. The wave functions of the Cu(111) surface extend more into the vacuum than the *h*-BN wave functions, implying that the overlap affects the former over a larger region than the latter, and that the effects of exchange repulsion are larger on the Cu(111) side than on the *h*-BN side.

This asymmetric depletion/accumulation pattern results in a net interface dipole that points out of the Cu(111) surface. Compared to the clean Cu(111) surface, adsorption of *h*-BN pushes back some of the electrons that would otherwise spill out into the vacuum. The potential step ΔV_{AS} is downwards going from Cu(111) to *h*-BN, so exchange repulsion *reduces* the work function with respect to the clean metal. Such a decrease is commonly found, not only in the physisorption of *h*-BN on other metal substrates (see below), but also in the physisorption of graphene, and of organic molecules. The shape of the electron displacement $\Delta\bar{n}_{AS}$ depends only weakly on the separation d of the *h*-BN plane from the Cu(111) surface while its amplitude decreases exponentially with increasing separation.

Exchange repulsion accounts for most of the potential step at distances around the equilibrium separation, but $\Delta\bar{n}_{AS}$ is not identical to $\Delta\bar{n}_{SCF}$, see Fig. 2 (c)-(d). The difference $\Delta\bar{n}_{diff} = \Delta\bar{n}_{SCF} - \Delta\bar{n}_{AS} = \bar{n}_{SCF} - \bar{n}_{AS}$ measures how the orbitals change as a result of chemical and vdW interactions. For all separations, $\Delta\bar{n}_{diff}$ describes an accumulation of electrons between the Cu(111) surface and the *h*-BN plane accompanied by a depletion of electrons in the Cu(111) surface and the *h*-BN plane, see Fig. 2(c)-(d). Such a depletion/accumulation pattern is typical of bond formation. At short distances, $d < 3\text{\AA}$, $\Delta\bar{n}_{diff}$ gives a sizable dipole opposite to that calculated from exchange repulsion. Interpreting $\Delta\bar{n}_{diff}$ as bond formation, the polarity of the bond is then such that *h*-BN is on the negative side, which is consistent with the fact that *h*-BN is more electronegative than Cu. The result is that $\Delta V_{SCF} < \Delta V_{AS}$.

Remarkably, at distances around the equilibrium separation 3.3\AA , $\Delta\bar{n}_{diff}$ shows a pattern that is fairly symmetric with respect to Cu(111) and *h*-BN, such that the

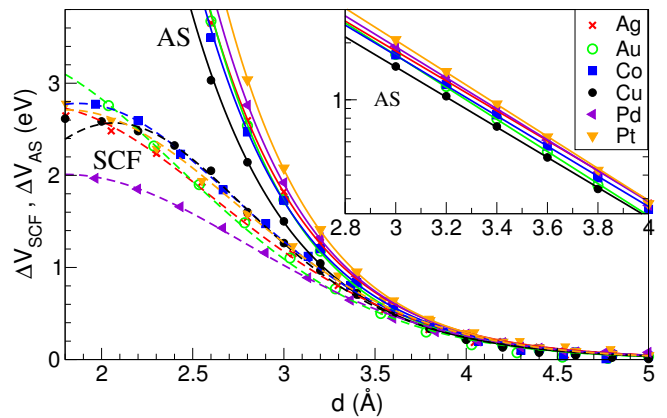


FIG. 4. (color online) Potential steps ΔV_{SCF} and ΔV_{AS} at metal|*h*-BN interfaces from self-consistent LDA calculations and the corresponding AS states, respectively. Inset: ΔV_{AS} on a logarithmic scale.

resulting dipole is moderate and results in $\Delta V_{SCF} \approx \Delta V_{AS}$. As $\Delta\bar{n}_{AS}$ goes to zero exponentially as a function of d , $\Delta\bar{n}_{diff}$ approaches $\Delta\bar{n}_{SCF}$ for large d . The electron displacement coming from the vdW bond is the only term remaining at these distances, but it yields only a small potential step.

Interface potential steps.—Fig. 4 shows the potential steps as a function of d at metal|*h*-BN interfaces for six different metal substrates. At $d \approx 3.5\text{\AA}$ the curves for the self-consistent potential steps, ΔV_{SCF} , converge with those of the exchange repulsion potential steps, ΔV_{AS} . At such separations the exchange repulsion is the dominant contribution to the interface potential steps. Although the electron displacement coming from the vdW bond has the longest range, it does not yield a sizable potential step. At $d < 3.0\text{\AA}$ interactions become stronger, and the contribution to the potential step of the electron displacement resulting from chemical bonds is not negligible. Compared to exchange repulsion only, this contribution tempers the potential steps for all metals considered.

The exchange repulsion potential steps exhibit an exponential behavior, $\Delta V_{AS}(d) \approx a_0 e^{-\gamma d}$, see the inset to Fig. 4. There is a correlation between the exponent γ and the work function W of the metal, i.e., γ increases if W increases. The correlation is weak, however, with γ varying between 1.82 for Ag and 1.95 for Pt. It is then not surprising that a single, average γ gives a reasonable fit for the curves of all metals. As the exchange repulsion gives the largest contribution to it, we can express the self-consistent potential step about the equilibrium separation as $\Delta V_{SCF} \approx f(d)e^{-\gamma d}$ where $f(d)$ can be described by a simple polynomial [10, 11].

Summary.—We have explored the formation of potential steps at metal|insulator interfaces, using metal|*h*-BN interfaces as archetypal example. Such potential steps can be surprisingly large, i.e., in excess of 1 eV, even when the bonding is weak, van der Waals bonding. Con-

structing a model for the Pauli exchange repulsion at the interface, we identify the major contributions to the interface potential steps. For metal-insulator separations that are typical for physisorption, exchange repulsion is the main origin of the interface potential step. At these and larger separations, van der Waals interactions are important to describe bonding, but give a relatively small contribution to the potential step. At shorter distances

chemical bonding interactions tend to reduce the interface potential step.

Acknowledgment.—M.B. acknowledges support from the European project MINOTOR, Grant No. FP7-NMP-228424. The use of supercomputer facilities was sponsored by the Physical Sciences (Exacte Wetenschappen) division of NWO (Nederlandse Organisatie voor Wetenschappelijk Onderzoek).

-
- [1] R. T. Tung, *Appl. Phys. Rev.* **1**, 011304 (2014).
- [2] A. K. Geim and I. V. Grigorieva, *Nature* **499**, 419 (2013); I. Popov, G. Seifert, and D. Tománek, *Phys. Rev. Lett.* **108**, 156802 (2012); W. Chen, E. J. G. Santos, W. Zhu, E. Kaxiras, and Z. Zhang, *Nano Letters* **13**, 509 (2013); C. Gong, L. Colombo, R. M. Wallace, and K. Cho, *Nano Letters* **14**, 1714 (2014); J. Kang, W. Liu, D. Sarkar, D. Jena, and K. Banerjee, *Phys. Rev. X* **4**, 031005 (2014).
- [3] C. R. Dean, A. F. Young, I. Meric, C. Lee, L. Wang, S. Sorgenfrei, K. Watanabe, T. Taniguchi, P. Kim, K. L. Shepard, and J. Hone, *Nature Nanotechnology* **5**, 722 (2010).
- [4] A. Nagashima, N. Tejima, Y. Gamou, T. Kawai, and C. Oshima, *Surface Science* **357-358**, 307 (1996).
- [5] A. B. Preobrajenski, A. S. Vinogradov, and N. Mårtensson, *Surface Science* **582**, 21 (2005).
- [6] D. Leuenberger, H. Yanagisawa, S. Roth, J. Osterwalder, and M. Hengsberger, *Phys. Rev. B* **84**, 125107 (2011).
- [7] S. Joshi, D. Eciya, R. Koitz, M. Iannuzzi, A. P. Seitsonen, J. Hutter, H. Sachdev, S. Vijayaraghavan, F. Bischoff, K. Seufert, J. V. Barth, and W. Auwärter, *Nano Letters* **12**, 5821 (2012).
- [8] T. Olsen, J. Yan, J. J. Mortensen, and K. S. Thygesen, *Phys. Rev. Lett.* **107**, 156401 (2011).
- [9] D. Stradi, S. Barja, C. Díaz, M. Garnica, B. Borca, J. J. Hinarejos, D. Sánchez-Portal, M. Alcamí, A. Arnau, A. L. Vázquez de Parga, R. Miranda, and F. Martín, *Phys. Rev. Lett.* **106**, 186102 (2011).
- [10] G. Giovannetti, P. A. Khomyakov, G. Brocks, V. M. Karpan, J. van den Brink, and P. J. Kelly, *Phys. Rev. Lett.* **101**, 026803 (2008); P. A. Khomyakov, G. Giovannetti, P. C. Rusu, G. Brocks, J. van den Brink, and P. J. Kelly, *Phys. Rev. B* **79**, 195425 (2009).
- [11] M. Bokdam, P. A. Khomyakov, G. Brocks, Z. Zhong, and P. J. Kelly, *Nano Letters* **11**, 4631 (2011); M. Bokdam, P. A. Khomyakov, G. Brocks, and P. J. Kelly, *Phys. Rev. B* **87**, 075414 (2013).
- [12] J. Gebhardt, F. Viñes, and A. Görling, *Phys. Rev. B* **86**, 195431 (2012).
- [13] A. Nagashima, N. Tejima, Y. Gamou, T. Kawai, and C. Oshima, *Phys. Rev. Lett.* **75**, 3918 (1995).
- [14] F. Schulz, R. Drost, S. K. Hämäläinen, T. Demonchaux, A. P. Seitsonen, and P. Liljeroth, *Phys. Rev. B* **89**, 235429 (2014).
- [15] G. Brocks, J. Tennyson, and A. van der Avoird, *J. Chem. Phys.* **80**, 3223 (1984); G. Brocks and A. van der Avoird, *Mol. Phys.* **55**, 11 (1985).
- [16] M. J. Dresser, T. E. Madey, and J. T. Yates, *Surface Science* **42**, 533 (1974); P. S. Bagus, V. Staemmler, and C. Wöll, *Phys. Rev. Lett.* **89**, 096104 (2002); H. Vázquez, Y. J. Dappe, J. Ortega, and F. Flores, *J. Chem. Phys.* **126**, 144703 (2007); P. S. Bagus, D. Käfer, G. Witte, and C. Wöll, *Phys. Rev. Lett.* **100**, 126101 (2008); L. Vitali, G. Levita, R. Ohmann, A. Comisso, A. D. Vita, and K. Kern, *Nature Materials* **9**, 320 (2010); P. C. Rusu, G. Giovannetti, C. Weijtens, R. Coehoorn, and G. Brocks, *Phys. Rev. B* **81**, 125403 (2010).
- [17] J. Neugebauer and M. Scheffler, *Phys. Rev. B* **46**, 16067 (1992).
- [18] J. Gómez Díaz, Y. Ding, R. Koitz, A. P. Seitsonen, M. Iannuzzi, and J. Hutter, *Theor. Chem. Acc.* **132**, 1350 (2013).
- [19] M. Bokdam, G. Brocks, M. I. Katsnelson, and P. J. Kelly, *Phys. Rev. B* **90**, 085415 (2014).
- [20] G. Kresse and J. Hafner, *Phys. Rev. B* **47**, 558 (1993); G. Kresse and J. Furthmüller, *Phys. Rev. B* **54**, 11169 (1996); G. Kresse and D. Joubert, *Phys. Rev. B* **59**, 1758 (1999).
- [21] J. P. Perdew and A. Zunger, *Phys. Rev. B* **23**, 5048 (1981).
- [22] J. P. Perdew, K. Burke, and M. Ernzerhof, *Phys. Rev. Lett.* **77**, 3865 (1996).
- [23] M. Dion, H. Rydberg, E. Schröder, D. C. Langreth, and B. I. Lundqvist, *Phys. Rev. Lett.* **92**, 246401 (2004).
- [24] T. Thonhauser, V. R. Cooper, S. Li, A. Puzder, P. Hyldgaard, and D. C. Langreth, *Phys. Rev. B* **76**, 125112 (2007).
- [25] J. Klimeš, D. R. Bowler, and A. Michaelides, *Phys. Rev. B* **83**, 195131 (2011).
- [26] V. G. Ruiz, W. Liu, E. Zojer, M. Scheffler, and A. Tkatchenko, *Phys. Rev. Lett.* **108**, 146103 (2012).
- [27] T. Björkman, A. Gulans, A. V. Krasheninnikov, and R. M. Nieminen, *Phys. Rev. Lett.* **108**, 235502 (2012).
- [28] F. Mittendorfer, A. Garhofer, J. Redinger, J. Klimeš, J. Harl, and G. Kresse, *Phys. Rev. B* **84**, 201401 (2011).
- [29] M. Reguzzoni, A. Fasolino, E. Molinari, and M. C. Righi, *Phys. Rev. B* **86**, 245434 (2012).
- [30] K. Berland and P. Hyldgaard, *Phys. Rev. B* **87**, 205421 (2013).
- [31] Experiments concur that the interaction is weak but the binding separation has not been measured directly [5, 7, 32]; the value reported in Ref. [7] results from interpreting STM measurements with the help of DFT calculations.
- [32] S. Roth, F. Matsui, T. Greber, and J. Osterwalder, *Nano Letters* **13**, 2668 (2013).